Surface microstructured selective emitters for TPV systems

SURFACE MICROSTRUCTURED SELECTIVE EMITTERS FOR TPV SYSTEMS

Hitoshi SAI, Hiroo YUGAMI, Yasuhiro AKIYAMA, Yoshiaki KANAMORI, and Kazuhiro HANE
Graduate school of Engineering, Tohoku University, Aoba-ku, Sendai 980-8579, Japan

ABSTRUCT

Surface microstructured selective emitters for thermo-photovoltaic generators are fabricated with lithography and Si anisotropic etching techniques. Two-dimensional series of reverse-pyramid cavities are fabricated on the surface with the structural periods of 1.5 and 2.0 μm. Thermal radiation spectra of the emitters are measured at high temperatures and selective emission due to the surface microstructures is clearly observed. Numerical calculations based on rigorous coupled-wave analysis (RCWA) are also performed to predict spectral properties of the emitters. Experimentally observed emission peaks are well reproduced by the calculation. It is also expected from the calculation that the selective emission due to these microstructures will show little directionality. An evaluation of selective emission efficiency shows that microstructured selective emitters are effective to improve efficiencies of TPV generation systems.

INTRODUCTION

Recently, thermophotovoltaic (TPV) generation has been researched as a new power generation system using photovoltaic (PV) cells.[1] For last decade, selective emitters have been studied in order to improve the efficiency of TPV generation systems, emitters which emit most radiation into the sensitive region of PV cells.

There are several methods to fabricate selective emitters at present. One familiar method is using oxides of rare earth materials[2-4] such as erbia (Er_2O_3) and ytterbia (Yb_2O_3). Doubly or triply charged rare earth ions have strong absorption or emission bands originated from their peculiar electron structures. This kind of emitters have been studied and developed by many researchers in recent ten years, however, they have some drawbacks; the spectral position where strong emission bands appear is not controllable because it is unique to each kind of rare earths, and the width of the emission band is relatively narrow. Besides, their material is restricted to oxide ceramics or crystals whose thermal conductivity is low.

Another method is to use surface microstructures on emitter surfaces. Periodic microstructures vary emissive properties depending on their structural period (Λ), depth and shape. Microstructured selective emitters (MS emitters) have some advantages which rare earth selective emitters do not. First, MS emitters can be varied the position of emission band by artificial means, that is, by controlling Λ. Therefore MS emitters have a possibility to achieve better spectral matching for any kinds of PV cells in comparison with other selective emitters. The shape and depth are also controllable to modify emitters' performance. Moreover, MS emitters can be fabricated from a wide variety of materials according to the situation. However, few reports about MS emitters have been published until now as far as authors' knowledge, except that Heinzel et al. have reported on microstructured tungsten selective emitters.[5]

In this paper, we report on the emissive properties of the reverse-pyramid type microstructured selective (RPMS) emitters which are fabricated with Si wet etching. Λ is designed to 1.5 and 2.0 μm, which matches with the sensitive region of narrow bandgap PV cells, for example, GaSb and InGaAsSb.

EXPERIMENT

Sample preparation

The RPMS emitters are prepared by the following procedure. First, SiO_2 thin film is made on a 2-inch Si single crystalline wafer with (100) surface by oxidation. After a resist coating, micro-cross stripe pattern with the period of Λ is drawn on the resist film with high-speed electron beam (EB) lithography. This EB lithography can be replaced by photolithography. Then, the developed wafer is soaked in a hydrogen fluoride (HF) solution to remove the bare part of the SiO_2 film. Consequently, microstructured SiO_2 mask is fabricated on the Si wafer. Next, the developed resist is eliminated and the wafer is soaked in a tetramethylammonium hydroxide (TMAH) solution which etches Si selectively. Since the etching rate for (100) plane is about 200 times faster than that for (111) plane, TMAH also etches Si crystal anisotropically. As a result, the uncovered Si surface is etched into a reverse pyramid shape composed of four (111) surfaces. After etching the SiO_2 mask, finally, thin Pt layer is sputtered at a high temperature by laser ablation technique so as to enhance the effect of the microstructured surfaces. This fabrication process has been already widely applied for the texture surfaces on single crystalline PV cells, however, Λ of our samples are much smaller than that of the conventional texture surfaces.

A scanning electron microscope (SEM) image of the RPMS emitter (Λ = 2.0 μm) is shown in Figure 1. From the SEM observation, it is confirmed that the periodic 2D
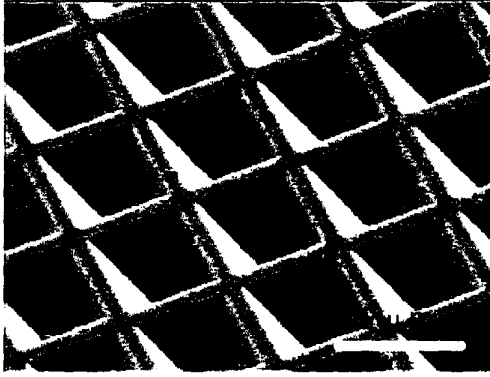
Fig. 1. An oblique view of the RPMS emitter with Λ = 2.0 μm obtained with a SEM.

series of reverse-pyramid cavity are fabricated on the Si surface without any disorders. The base length and depth of the pyramid are about 1.6 and 1.1 μm, respectively. These values are used in numerical calculations mentioned later.

Experimental apparatus

The apparatus used to measure emissive properties is consisted of three components, namely, a vacuum heater, blackbody furnace, and a Fourier-transform near-infrared spectrometer (FT-NIR). A Sample is heated by SiC electronic heater placed in a vacuum chamber which has a CaF_2 optical window. Thermal emission from a sample passes through the window and it enters into the FT-NIR. Measured spectra are converted into emissive power spectra possessing the absolute value by multiplying an apparatus coefficient spectrum which is measured with the blackbody furnace. Sample's temperature is measured with a thermocouple on its surface.

Calculation model

In order to simulate emissive properties of the RPMS emitters, we have performed rigorous coupled-wave analysis (RCWA),[6-8] which is a method to analyze the general three-dimensional grating diffraction problem by solving Maxwell's equations rigorously. Since it can treat periodic structures divided several layers in the direction of the depth, RCWA is a suitable calculation method to handle continuous gratings like the RCWA emitter. Input data are only the state of incident beam, the structural profiles and optical constants (n, k) of the gratings. In this study, diffraction efficiencies for each diffraction order are calculated.

In the calculation, we regard the microstructured surface as a multilevel grating consisted of ten binary layers with Pt coatings on their sides. At the substitution of optical constants of Si and Pt, we refer to the literature data.[9,10] The diffraction orders up to ±7th are considered for x- and y- directions, respectively, and hence diffraction
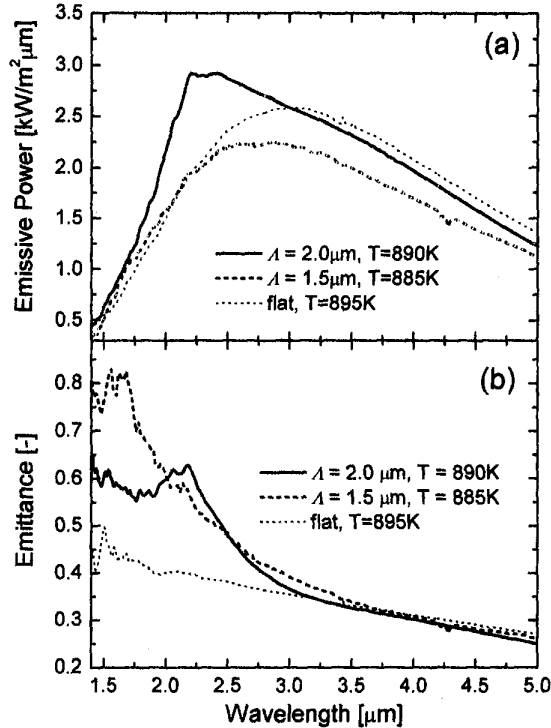

Fig. 2. Emissive properties of the RPMS emitters with Λ = 1.5 μm (dashed line) and 2.0 μm (solid line) and a flat emitter with Pt coating (dotted line). (a) measured emissive power spectra, (b) emittance spectra calculated from (a).

efficiencies for 225 diffraction orders are calculated for each wavelength (λ). We have checked that the calculation outputs sufficiently converge under these conditions.

RESULTS AND DISCUSSION

Figure 2(a) shows the normal emissive power spectra of the RPMS emitters with Λ = 2.0 μm measured at 890K and Λ =1.5 μm measured at 885K. As compared with a flat sample, both emitters show strong emission in shorter λ. These spectral alternations originate from the resonance effect between the emissive field and surface microstructures. Figure 2(b) shows emittance (ε) spectra calculated from Fig. 2(a). Selective emission peaks are clearly observed in the RPMS emitters' spectra. The peak positions are about 1.7 μm for Λ =1.5 μm and 2.2 μm for Λ = 2.0 μm, and therefore it is clarified that the emission peak position can be controlled by controlling the structural period Λ. Small dips which appear in λ < 2.0 μm are noise.

Using the RCWA technique, we calculate diffraction efficiencies up to ±7th diffraction orders. Absorptance α of the microstructured sample is estimated from the following equation,

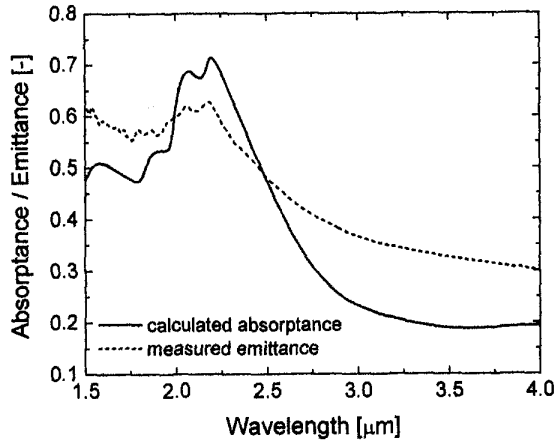$$\alpha(\lambda) = 1 - \sum_{i=-N}^{N}\sum_{j=-N}^{N}(DER_{i,j}(\lambda) + DET_{i,j}(\lambda)),$$

1017

Fig. 3. An absorptance spectrum of the RPMS emitter with Λ = 2.0 μm calculated by RCWA with θ = 5° and ψ = 45° (solid line). Dotted line is the same spectrum shown in Fig. 2(b).

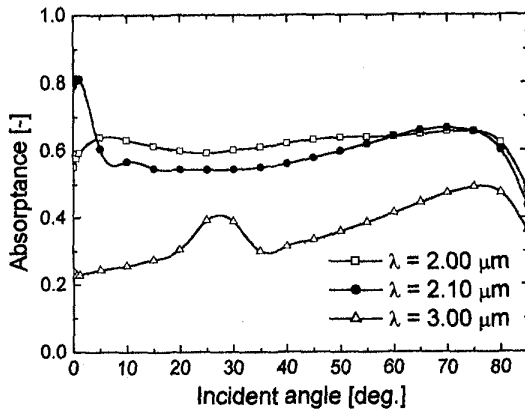Fig. 4. Incident angle dependence of the RPMS emitter's absorptance (Λ = 2.0 μm) calculated by RCWA with ψ = 0° as a function of λ.
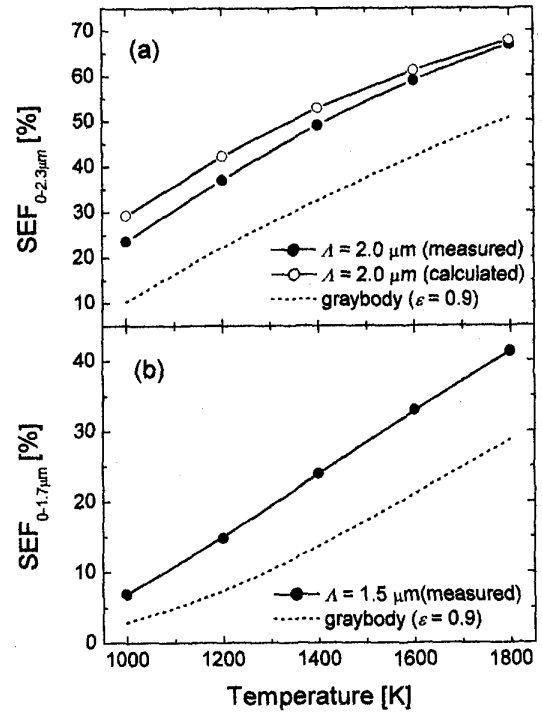

Fig. 5. Temperature dependence of selective emission efficiency (SEF) of the MS emitters. (a) SEF for InGaAsSb PV cells whose sensitive region are supposed to λ = 0 to 2.3 μm. (b) SEF for GaSb PV cells whose sensitive region are supposed to λ = 0 to 1.7 μm.

where $DER_{i,j}$ is the (i, j)th backward diffraction (refection) efficiency, $DET_{i,j}$ is the (i, j)th forward diffraction (transmission) efficiency, N is the maximum diffraction order considered in this calculation (here, N=7). On the assumption that the Kirchihoff's law is still satisfied in this case, α and ε are equal. Hereafter, therefore, we discussed about the calculated α and the measured ε. Figure 3 shows an α spectrum of the sample with Λ = 2.0 μm. The incident angle of the incident beam (θ) is set to 5° considering the expansion of the beam. The polarization angle (ψ) is set to 45° as a mean value because we have found from the calculation that the spectral shape at $\lambda \approx \Lambda$ varies smoothly in the range of ψ = 0° to 90°. An ε spectrum shown in Fig. 2(b) is also plotted in the figure. The overall feature of the calculated α is almost consistent with that of the measured ε. Especially the main peaks at λ = 2.0 and 2.2 μm in the ε are well reproduced in the α. The

higher ε value in longer λ is expected to be due to the temperature dependence of (n, k). For an accurate calculation, (n, k) at high temperatures should be substituted into the RCWA calculation, however, we have used (n, k) at room temperature because there is no literature data about (n, k) at high temperatures. We have confirmed from the calculation based on the Drude model[11] that α increases with increasing temperature. This fact may support the speculation mentioned above. Surface roughness on the samples is also considered as another reasons of high ε.

Figure 4 shows the incident angle dependence of α for the sample of Λ = 2.0 μm. This is obtained by RCWA calculation with ψ = 0°. In the resonance region ($\lambda \approx \Lambda$) such as λ = 2.0 or 2.1 μm, α varies sharply for $\theta \approx 0°$, while it hardly changes for θ > 5°. In the case of $\lambda > \Lambda$ such as λ = 3.0 μm, on the other hand, α increases gradually in proportion to θ. There is a peak at θ = 27°, but its origin has been not confirmed yet. We believe that it is a weak resonance of the lateral component of the incident beam. From Fig. 4, it is revealed that α at λ = 2.0 and 2.1 μm ($\lambda \approx \Lambda$) are higher than that at λ = 3.0 μm for any value of θ. From this results, it is strongly suggests that the RPMS emitters show strong selective emission in the wide range of the angle that radiation beam is emitted.

Selective emission efficiency (SEF) is often used to

estimate the performance of selective emitters, and then we apply SEF to the RPMS emitters. Generally, SEF is defined as the ratio of the power emitted in the PV cell's sensitive region to the total emissive power.[11] The RPMS emitters' SEFs are calculated by multiplying the measured ε or calculated α (only for $\Lambda = 2.0$ μm, $\theta = 5°$, $\psi = 45°$) and the blackbody radiation, changing temperature. In this estimation we use the ε shown in Fig. 2(b) for all temperature, assuming it hardly depend on temperature.

Figure 5(a) shows the SEF for InGaAsSb PV cells, whose sensitive region is supposed to $\lambda = 0$ to 2.3 μm, as a function of temperature. The SEF of the RPMS emitter with $\Lambda = 2.0$ μm are 16 ~ 20% higher than that of a graybody emitter with $\varepsilon = 0.9$ for all temperatures shown in the figure. A similar plot for GaSb PV cells, whose sensitive region is supposed to $\lambda = 0$ to 1.7 μm, is shown in Fig. 5(b). The SEF of the RPMS emitter ($\Lambda = 1.5$ μm) is also 5 ~ 14% higher than that of a graybody. These values will be improved by optimizing the shape and material.

CONCLUSIONS

Reverse-pyramid type microstructured selective emitters have been fabricated with Si anisotropic etching. The structural periods of the microstructures are 1.5 μm and 2.0 μm, which is matching with GaSb or InGaAsSb photovoltaic cells. Their emissive spectra have been measured and selective emission due to the resonance effect has been clearly observed. It is confirmed that the position of the selective emission varies with the structural period. Numerical calculations based on rigorous coupled-wave analysis have been carried out and the results agree well with the measured data. It is also suggest from the calculation that these emitters are expected to show selective emission with a little directionality. Our evaluation of selective emission efficiency shows that the microstructured emitter is a promising option to obtain high efficiency TPV systems.

ACKNOWLEDGEMENTS

REFERENCES

[1] T. J. Coutts, "A Review of Progress in Thermophotovoltaic Generation of Electricity," *Renew. Sustain. Energy Rev.* **3**, 1999, pp. 77-184.

[2] D. L. Chubb, A. T. Pal, M. O. Patton, and P. P. Jenkins, "Rare Earth Doped High Temperature Ceramic Selective Emitters," *J. Eu. Ceram. Soc.* **19**, 1999, pp. 2551-2562.

[3] M. G. Krishna, M. Rajendran, D. R. Pyke, and A. K. Bhattacharya, "Spectral Emissivity of Ytterbium Oxide-based Materials for Application as Selective Emitters in Thermophotovoltaic Deveices," *Sol. Energy Mater. Sol. Cells* **59**, 1999, pp. 337-348.

[4] H. Sai, H. Yugami, K. Nakamura, N. Nakagawa, H. Ohtsubo, and S. Maruyama, "Selective Emission of $Al_2O_3/Er_3Al_5O_{12}$ Eutectic Composite for Thermophoto-voltaic Generation of Electricity," *Jpn. J. Appl. Phys.* **39**, 2000, pp. 1957-1961.

[5] A. Heinzel, V. Boerner, A. Gombert, V. Witter, and J. Luther, "Microsturctured Tungsten Surfaces as Selective Emitters," *Proc. Thermophotovoltaic Generation of Electricity 4th NREL Conf. Denver, Colorado, 1998*, ed. T. J. Coutts, J. P. Benner and C. S. Allman (AIP, New York, 1999) pp. 191-196.

[6] M. G. Moharam, "Coupled-Wave Analysis of Two-Dimensional Dielectric Gratings," *Proc. Soc. Photo-Opt. Instrum. Eng.* **883**, 1988, pp. 8-11.

[7] S. Peng and G. M. Morris, "Efficient implementation of rigorous coupled-wave analysis," *J. Opt. Soc. Am. A* **12**, 1995, pp.1087-1096.

[8] Y. Kanamori, H. Kikuta, and K. Hane, "Broadband Antireflection Gratings for Glass Substrates Fabricated by Fast Atom Beam Etching," *Jpn. J. Appl. Phys.* **39**, No.7B, 2000, pp. L735 - L737.

[9] D. W. Lynch and W. R. Hunter, *Handbook of Optical Constants of Solids I*, E. D. Palik, ed. (Academic Press, New York,. 1985), pp.333-341.

[10] D.F. Edwards, *Handbook of Optical Constants of Solids I*, E. D. Palik, ed. (Academic Press, New York) 1985, pp.547-569.

[11] K. Ujihara, "Reflectivity of Metals at High Temperatures," *J. Appl. Phys.* **43**, No. 5, 1972, pp. 2376-2382.